

High-pressure structural properties of anthracene up to 10 GPa

Martin Oehzelt* and Roland Resel

Institute of Solid State Physics, Graz University of Technology, Petersgasse 16, 8010 Graz, Austria

Atsuko Nakayama

National Institute of Advanced Industrial Science and Technology, AIST Central 5, 1-1-1 Higashi, Tsukuba, Ibaraki 305-8565, Japan

(Received 25 June 2002; published 11 November 2002)

This study concentrates on the crystal structure of anthracene ($C_{14}H_{10}$) under high pressure as a representative of the polyacene family. Angle-dispersive x-ray diffraction experiments from crystalline powder were performed using synchrotron radiation and a diamond anvil cell with a pressure-transmitting medium to keep hydrostatic condition. The structural data were analyzed by Rietveld refinements to obtain molecular arrangements and lattice parameters as a function of pressure up to 10.2 GPa. The lattice parameters a , b , and c decrease by 1.19 Å (−13.9%), 0.53 Å (−8.8%), and 0.68 Å (−6.1%), respectively, while the monoclinic angle β increases by 2.5° in this pressure region. The layer distance is also significantly decreased by 0.83 Å (−9.0%). The detailed analysis of the arrangement of the molecules within the crystal structure reveals that the molecular planes become more and more parallel relative to each other. The closest intermolecular distance decreases from 3.6 Å at ambient pressure to 2.8 Å (−22.0%) at 10.2 GPa.

DOI: 10.1103/PhysRevB.66.174104

PACS number(s): 61.10.Nz, 64.30.+t, 61.50.Ks, 71.20.Rv

I. INTRODUCTION

Electro-active organic materials based on conjugated molecules like the polyacene family show outstanding optical and electronic properties combined with high charge carrier mobilities.^{1–4} Significant insights into the electronic and optical properties of those materials can be gained by studying isolated molecules. For instance, optical absorption and luminescence properties can be qualitatively well understood in terms of the delocalized π -electron systems that are typical for these conjugated molecules.⁵ However, effects of intermolecular interactions, inherently present in the solid state, are neglected in such an approach. Transport properties such as the carrier mobilities are determined by the overlap of wave functions on neighboring molecules: also, optical features such as the luminescence quantum yield can be drastically changed in the solid state as compared to molecules in solution.^{6–9} The goal of this work is to investigate the structural changes and intermolecular interactions by applying hydrostatic pressure, because an understanding of the electro-optical features is only possible with a detailed knowledge of the crystal structure including the molecular orientations relative to each other and the distances between them. The high-pressure technique is a very powerful tool to probe intermolecular properties without changing the chemical composition. The resulting change of the intermolecular alignment and distances modulates the physical properties of the material. Especially in pentacene the pressure-induced increase of the intermolecular overlap results in a vanishing of the band gap and at 27 GPa (for single crystal) and 36 GPa (for powder), and a pressure-induced metalization¹⁰ was observed. The band structure of this metallic phase is still complex with large anisotropies.

Organic molecular crystals are characterized by two different interactions between the atoms. On the one hand, there are strong covalent interactions between atoms within a single molecule and, on the other hand, there are weak van

der Waals forces between the molecules. As a result of this fact, the molecules are rigid compared to their intermolecular bonding. The anthracene molecules have planar conformation. Anthracene crystallizes in the monoclinic space group $P2_1/a$ (Ref. 11) with unit-cell parameters at ambient pressure and temperature of $a=8.553$ Å, $b=6.016$ Å, $c=11.172$ Å, and $\beta=124^\circ, 60'$.¹² There are two molecules per unit cell located at 000 and $0\frac{1}{2}$. These molecules are translationally inequivalent and are arranged in layers. Within these layers the molecules are twisted to each other (see Fig. 1).¹³ This alignment is the so-called herringbone structure. The upper two molecules in Fig. 1 belong to one layer, whereas the lower molecule is already in the next.

II. EXPERIMENTAL TECHNIQUES

Anthracene powder was purchased from Aldrich Ltd. with a purity of 99+%. Analyzing the powder by mass spectroscopy

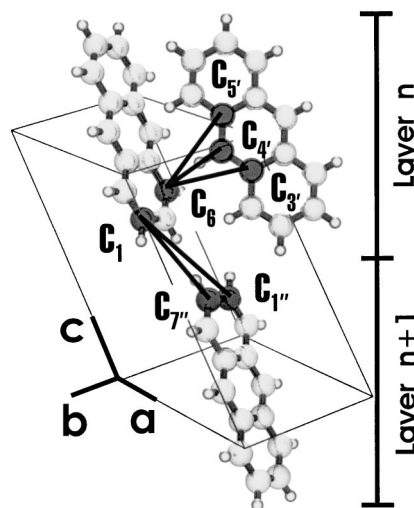


FIG. 1. Crystal structure of anthracene. The thin solid lines indicate the unit cell; the other lines show intermolecular distances.

copy revealed that the purity is better than 99.9%. The anthracene powder was manually ground in an agate mortar. The particle size of the powder was regularly checked by an optical microscope in order to obtain an average size of 1 μm . Totally, the grinding procedure took 6 h. Subsequently, the powder was heat treated at 80 °C for 2 h in order to reduce microstrains induced by the mechanical treatment. A careful powder preparation is mandatory for x-ray powder diffraction, since randomly orientated crystallites with good statistics and defined granularity of these crystallites are required.

High pressures up to 10 GPa were applied using a diamond anvil cell (DAC). The culet sizes of the diamond anvils were 500 μm , and the diameter of the stainless-steel gasket hole was 180 μm . The gasket was mounted on the culet of one diamond anvil, and the powder was filled into the gasket hole. In order to guarantee hydrostatic pressure during the experiments a methanol-ethanol mixture (4:1 by volume) was used as pressure-transmitting medium. Note that methanol-ethanol loses hydrostaticity at around 10 GPa.^{14,15} The pressure in the gasket hole was determined by the fluorescence of ruby.¹⁶

Angle-dispersive x-ray diffraction (ADX) in Debye-Scherrer geometry was performed at the beamline BL-18C, Photon Factory, KEK, Tsukuba, Japan. Highly collimated monochromatic synchrotron radiation with a wavelength of 0.9204 Å (13.4698 keV) was used. The beam diameter was 100 μm to avoid any contact of the x-ray beam with the gasket. An imaging plate with a resolution of 100 \times 100 μm^2 and a size of 2000 \times 2500 pixels was used as detector. The exposure time was 45 min for a single experiment. Diffraction patterns were taken up to 14.3 GPa in steps of 1 GPa. Subsequently, the reversibility of the pressure-induced effects on anthracene was verified by releasing the pressure and taking diffraction patterns at 8.7 GPa, 4.4 GPa, and ambient pressure. As a consequence of the careful sample preparation, homogeneous Debye-Scherrer rings were observed. Integration along the Debye-Scherrer rings was performed using the software PIP (Ref. 17) in order to obtain a total intensity as a function of the scattering angle 2θ .

These data were analyzed by Rietveld refinement using the software package GSAS.¹⁸ The number of degrees of freedom was decreased by applying a rigid-body approximation: the molecules are assumed to have fixed shape, but they can change their relative orientation.^{19,20} The geometry of the anthracene molecule was taken from ambient-pressure single-crystal data and remained unchanged over the whole pressure region. The background fit was done manually, but was not removed in the fitting process; Pseudo-Voigt functions were used as the peak profile, and no preferred orientation was considered. Besides the standard parameters (zero, scaling factor) also the profile function parameters GU , GV , GW , GP , and LX and crystal structure parameters of anthracene were refined.

The pattern at 0 GPa was refined using starting parameters of the known single-crystal structure. The parameters obtained from this procedure are taken as input for the refinement of the next pressure point. The quality of the fit was

TABLE I. Reduced least-squares sum χ^2 , weighted R_p value, and the structure factor R_{F2} value for all measured pressure points.

p [GPa]	χ^2	R_{wp}	R_{F2}
0.16	0.0894	0.0130	0.1127
1.05	0.2854	0.0141	0.1510
2.45	0.1330	0.0164	0.1548
3.07	0.1480	0.0165	0.1440
4.04	0.1761	0.0130	0.1619
5.05	0.0978	0.0141	0.0872
6.07	0.2133	0.0154	0.1683
7.06 ^a	0.9663	0.0181	0.2593
8.02	0.0681	0.0131	0.1232
9.01	0.0951	0.0141	0.1183
10.20	0.1512	0.0105	0.1018
8.70 ^b	0.2019	0.0166	0.3074
4.37 ^b	0.1673	0.0163	0.1877
0.00 ^{b,c}	0.0832	0.0155	0.1804

^aIncluding gasket peaks.

^bDecreasing pressure.

^cOpen cell.

rated by the reduced χ^2 , the weighted R_p value without background, and the structure factor R_{F2} value.

III. EXPERIMENTAL RESULTS

The described refinement strategy was applied to the observed diffraction pattern at each pressure point. Table I shows the quality factors of the fits. At 7 GPa the incident beam hit the gasket and a single additional peak was recorded. This explains the lower-quality factors at 7 GPa. Subsequently, the beam was readjusted, which improved the experiment and furthermore the quality factors. Figure 2 shows the result of the refining process for 0.2, 5.1, and 10.2 GPa. The crosses symbolize the experimental values, the line shows the calculated pattern, and the difference between both is given by the solid line below. 2θ angles of the three patterns range from 5° to 28°. Especially for the peak 001 at around 6° and for the double peak 200, $\bar{2}$ 11 at around 16° the shift with pressure can be seen. The very broad peak in the background at around 14° 2θ at 0.2 GPa that shifts to around 18° 2θ originates from the methanol-ethanol pressure medium. Additional background measurements of the pressure-transmitting medium have proved this fact.

The Rietveld refinement reveals the lattice constants of anthracene as a function of pressure. The result is illustrated in Fig. 3. As expected, the lattice parameters a , b , and c decrease with increasing pressure. The monoclinic angle β increases. It is remarkable that the pressure dependence of the lattice constant a is approximately twice as high as the change of the two other lattice constants b and c . Up to a pressure of 10.2 GPa the lattice constant a is reduced by 1.3 Å, while b and c change only by 0.6 and 0.7 Å, respectively. The monoclinic angle β increases by 3.3° in the same pressure region. These results are in very good agreement with

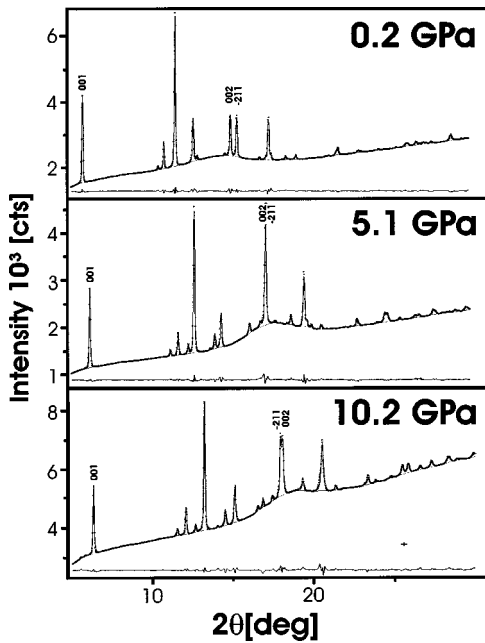


FIG. 2. Measured (crosses) and refined (solid lines) diffraction pattern of anthracene at 10.2 GPa. The difference between measurement and fit is shown below. The inset is a zoom at higher 2θ angles.

the literature data. However, data are known only up to 0.6 GPa,²¹ 1.0 GPa,²² and 2.5 GPa.²³

With knowledge of the lattice parameter under pressure it is possible to give an equation of state (EOS). For anthracene crystals the Vinet-type EOS (Ref. 24) was used to obtain the bulk modulus and its derivative. It is standard to use this parametric EOS for aromatic molecular crystals.²⁵ Figure 4 shows the fit to the observed unit-cell volume under pressure. The volume decreases by 28%. The bulk modulus at ambient pressure and temperature is $B_0 = (6.08 \pm 0.24)$ GPa and its derivative is $B'_0 = 9.78 \pm 0.27$. These values are in

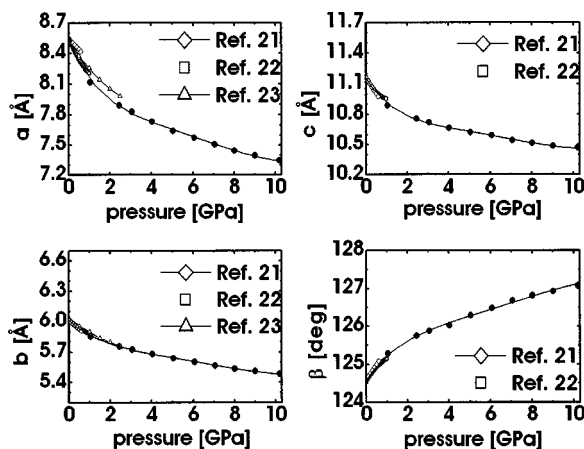


FIG. 3. Pressure dependence of the unit-cell parameters a , b , c , and β of this work (solid lines and dots) compared to the literature data (Refs. 21–23).

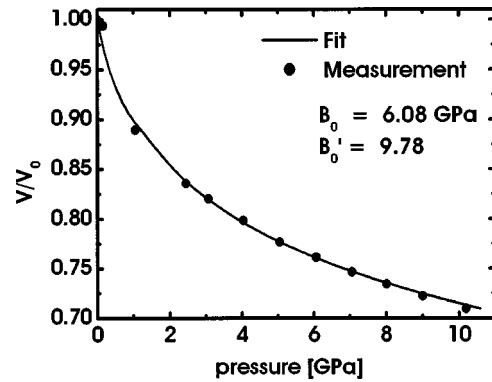


FIG. 4. Volume compressibility of anthracene at room temperature. The solid line is the fit of the Vinet-type equation of state.

agreement with prior determinations, which were in the range of 6.5–7.5 GPa for B_0 and 7.3 to 9.8 for B'_0 .²⁶

The alignment of the anthracene molecules within the crystal structure is described by three different orientation angles. The definitions of these angles are given in the right part of Fig. 5. The herringbone angle θ is the angle between the normal vectors (vectors perpendicular to the molecular planes) of neighboring molecules. The tilting angle of the long molecular axis with respect to the vector perpendicular to the ab plane of the unit cell is denoted by χ . The angle between the long molecular axes of two translational inequivalent molecules is named δ . These three angles are determined from single-crystal data at ambient pressure; the values are $\theta = 128.5^\circ$, $\chi = 30.7^\circ$, and $\delta = 14.3^\circ$. From our refinement of the diffraction pattern at 0.2 GPa we get the following values: $\theta = 124.5^\circ$, $\chi = 30.0^\circ$, and $\delta = 12.4^\circ$. The pressure dependence of these three angles is given in Fig. 5. The biggest change is observed in case of the herring-

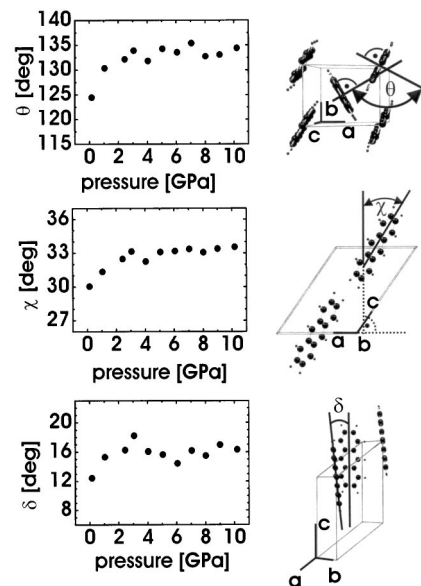


FIG. 5. Right side: the three angles θ , χ , and δ describe the orientation of the anthracene molecules within the crystal structure. Left side: the pressure dependence of these angles.

bone angle θ , which increases by 12° . The angles χ and δ show a smaller dependence with pressure, with 4° and 6° , respectively.

At pressures higher than 10 GPa the onset of a crystallographic phase transition is observed. New diffraction peaks appear at low angles. Therefore only data up to a pressure of 10 GPa are presented in this work. To confirm the reversibility the pressure was released after reaching the maximum pressure. The obtained results fit well to the presented lattice constants and orientation angles for raising pressure.

IV. DISCUSSION

According to the results of this analysis, there is no evidence of a structural phase transition up to 10 GPa at room temperature. All structural parameters have smooth pressure dependences. The layer distance decreases from 9.18 to 8.35 Å by 0.83 Å between ambient pressure and 10.2 GPa. The magnitude of this change is remarkably high and is a result of the decrease of c together with an increase of β . This behavior seems to be the explanation why the angle δ slightly increases, which is not obvious. In the terms of the closed packing principle²⁷ it would be expected that δ decreases to zero, but the molecules of one layer are forced into the next layer and have to rearrange in this way. Also, a consequence of the decrease of the layer distance is the slight increase of the angle χ .

The change of the lattice parameter a under pressure is twice as high as the lattice parameter b . This fact leads to the increase of the herringbone angle θ . It is clear that the molecules have to rearrange at most in the direction of a and the molecular planes of two neighboring molecules become more and more parallel within the herringbone pattern. Generally, it can be concluded that the biggest changes of the orientation angles occur at pressures up to 3 GPa. Figure 4 shows that the compressibility of anthracene decreases with increasing pressure. This fact can also be proved by a decrease of the pressure dependence of the lattice parameter in Fig. 3. These smaller changes of the unit-cell parameters result in a weaker rearrangement of the molecules at higher pressure.

Low temperature has comparable effects to the crystal structure as the influence of pressure. Both decrease the unit-cell volume. So it is not surprising that single-crystal investigations performed down to 94 K (Ref. 12) yield a similar temperature dependence of the lattice parameters when compared to the pressure dependence up to approximately 0.3 GPa. These single-crystal solutions show that the molecular arrangements have the same tendencies as shown in this high-pressure study (all three orientation angles increase). A change of the conformation of the anthracene molecule is not detectable.

To show the significance of the Rietveld refinement interatomic distances between neighboring molecules are plotted in Fig. 6. The carbon atoms are labeled in the same way as depicted in Fig. 1. The dashed line marks the doubled van der Waals radius of a carbon atom²⁷ (1.8 Å) at ambient pressure and temperature. At ambient pressure all carbon distances are larger than this value. With increasing pressure the

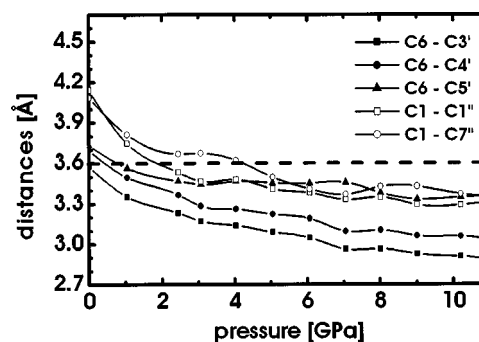


FIG. 6. Intermolecular carbon distances as a function of pressure of the distances given in Fig. 1 (for an explanation see text).

interatomic C-C distances decrease. Solid symbols characterize interatomic distances between molecules within the herringbone structure. Open symbols show the pressure dependence between two layers. It is remarkable that the decrease of the distances are smooth curves. This behavior is not obvious because the refinement only tries to fit a calculated pattern to the observed pattern by refining the structure. Unphysical atomic positions and distances could occur from the Rietveld refinement as there are no interatomic forces considered. This fact indicates the success of the refining procedure and illustrates the quality of the fit.

High-pressure measurements of fused-ring aromatic compounds showed that dimerization and polymerization processes cannot be neglected in general^{10,28-31} especially as there is a negative activation enthalpy of dimerization under pressure observed in anthracene.³⁰ These reactions could cause irreversible changes of the diffraction pattern. In our case, up to 10.2 GPa there is no evidence of such effects because with decreasing pressure reversible structural data were obtained.

One interesting effect was observed during application of pressure: under the microscope a color change was observed. At ambient pressure the anthracene powder appears transparent. With increasing pressure the color changes from white, yellow, orange, red, and finally to almost black. This color change can be explained by a redshift of the absorption peaks as a function of pressure which was already experimentally observed³² as well as theoretically considered.³³

V. CONCLUSION

Using high-quality diffraction data in combination with a Rietveld refinement algorithm, it is possible to obtain the molecular orientation in organic crystals from powder diffraction experiments as a function of pressure. These results can only be obtained with the rigid-body approximation which works good for rigid aromatic molecules like anthracene. In the case of anthracene the lattice parameter a changes twice as much as b or c . The difference in the changes is the reason for a reorientation in the herringbone pattern where neighboring molecules become more and more

parallel. In general, the reorientation of the molecules represented by the three orientation angles is gradually with magnitudes around 10° or less. These data can be used as input parameter for *ab initio* band structure calculations which predict the change of optical and electrical properties under pressure.

ACKNOWLEDGMENTS

This research project is supported by the Austrian Science Fund (Project No. P14237-PHY) and the foreign affairs division of the Graz University of Technology. And finally thanks to Georg Heimel for helpful discussions.

*Corresponding author. Electronic address: martin.oehzelt@tugraz.at

- ¹*Numerical Data and Functional Relationships in Science and Technology*, edited by O. Madelung, Landolt-Börnstein, New Series, Group III, Vol. 17, Pt. a (Springer-Verlag, Berlin, 1982).
- ²C. D. Dimitrakopoulos, A. R. Brown, and A. Pomp, *J. Appl. Phys.* **80**, 2501 (1996).
- ³J.-J. Lin, D. J. Gundlach, S. Nelson, and T. N. Jackson, *IEEE Electron Device Lett.* **18**, 606 (1997).
- ⁴Gilles Horowitz, *Adv. Mater.* **10**, 365 (1998).
- ⁵N. Nijegorodov, V. Ramachandran, and D. P. Winkoun, *Spectrochim. Acta, Part A* **53**, 1813 (1997).
- ⁶H. W. Offen, *J. Chem. Phys.* **44**, 699 (1966).
- ⁷P. F. Jones and Malcolm Nicol, *J. Chem. Phys.* **48**, 5440 (1968).
- ⁸A. Otto, R. Keller, and A. Rahman, *Chem. Phys. Lett.* **49**, 145 (1977).
- ⁹R. Sonnenstein, K. Syassen, and A. Otto, *J. Chem. Phys.* **74**, 4315 (1981).
- ¹⁰R. B. Aust, W. H. Bentley, and H. G. Drickamer, *J. Chem. Phys.* **41**, 1856 (1964).
- ¹¹R. Mason, *Acta Crystallogr.* **17**, 547 (1964).
- ¹²C. P. Brock and J. D. Dunitz, *Acta Crystallogr., Sect. B: Struct. Sci.* **46**, 795 (1990).
- ¹³G. R. Desiraju and A. Gavezzotti, *Acta Crystallogr., Sect. B: Struct. Sci.* **45**, 473 (1989).
- ¹⁴G. J. Piermarini, S. Block, and J. D. Barnett, *J. Appl. Phys.* **44**, 5377 (1973).
- ¹⁵K. Takemura, *J. Appl. Phys.* **89**, 662 (2001).
- ¹⁶H. K. Mao, J. Xu, and P. M. Bell, *J. Geophys. Res.* **91**, 4673 (1986).
- ¹⁷H. Fujihisa, computer program PIP, AIST, Tsukuba, Japan, 1995–2000.
- ¹⁸R. B. Von Dreele and A. C. Larson (unpublished).
- ¹⁹C. Scheringer, *Acta Crystallogr.* **16**, 546 (1963).
- ²⁰V. Schomaker and K. N. Trueblood, *Acta Crystallogr., Sect. B: Struct. Crystallogr. Cryst. Chem.* **24**, 63 (1967).
- ²¹S. Elnahwy *et al.*, *J. Chem. Phys.* **68**, 1161, 1 (1978).
- ²²R. Pufall and J. Kalus, *Acta Crystallogr., Sect. A: Found. Crystallogr.* **44**, 1059 (1988).
- ²³J. M. Léger and H. Aloualiti, *Solid State Commun.* **79**, 901 (1991).
- ²⁴P. Vinet, J. R. Smith, J. Farrante, and J. H. Rose, *Phys. Rev. B* **35**, 1945 (1987).
- ²⁵A. Nakayama, H. Fujihisa, K. Aoki, and R. P. Carlón, *Phys. Rev. B* **62**, 8759 (2000).
- ²⁶S. N. Vaidya and G. C. Kennedy, *J. Chem. Phys.* **55**, 987 (1971).
- ²⁷A. I. Kitaigorodsky, *Molecular Crystals and Molecules* (Academic, New York, 1973).
- ²⁸G. A. Samara and G. H. Drickamer, *J. Chem. Phys.* **37**, 474 (1962).
- ²⁹V. C. Bastron and H. G. Drickamer, *J. Solid State Chem.* **3**, 550 (1971).
- ³⁰R. B. Murphy and W. F. Libby, *J. Am. Chem. Soc.* **99**, 39 (1977).
- ³¹R. Engelke and N. C. Blais, *J. Chem. Phys.* **101**, 10961 (1994).
- ³²S. Wiederhorn and H. G. Drickamer, *J. Phys. Chem. Solids* **9**, 330 (1959).
- ³³K. Weinmeier, P. Puschnig, C. Ambrosch-Draxl, G. Heimel, E. Zojer, and R. Resel, MRS Symposia Proceedings No. 665 (Materials Research Society, 2001), C8.20.1.